DESIGN OF THREE-CHANNEL FILTER BANKS FOR LOSSLESS IMAGE COMPRESSION

Tilo Strutz

Deutsche Telekom AG, Hochschule für Telekommunikation
Institute of Communications Engineering
Gustav-Freytag-Str. 43-45, 04277 Leipzig, Germany

ABSTRACT

This paper proposes a novel design method for 3-channel filter banks based on the lifting scheme. The resulting filter bank is able to map integer signal values to integer sub-band values. The design also offers low-complexity handling of the signal boundaries. In application to image data compression, the new integer wavelet decomposition shows competitive performance compared to the reversible 5/3 transform used in JPEG2000.

***Index Terms*—** integer wavelet transform, filter design, lifting, image coding

1. INTRODUCTION

Wavelet transforms have found an application in many fields of signal processing and especially in image data compression [1].

The discrete wavelet transformation is typically performed via a cascade of two-channel filter banks leading to a dyadic decomposition of the signal following Mallat's principle [2]. The design of the corresponding filters has to ensure that the signal can be perfectly reconstructed, i.e. the design is subject to at least two conditions: zero signal distortion and complete cancelling of aliasing components [3]. The lifting scheme, introduced by Wim Sweldens [4], fulfils these conditions by definition and is therefore a handy tool for wavelet-filter design. Moreover, it has been proven that each two-channel filter bank can be converted into a lifting structure [5].

Figure 1 depicts the principle of lifting. Module S splits the signal into values at odd ($x[2n+1]$) and even positions ($x[2n]$). The values of the even path are fed into a prediction module P and the resulting prediction value is subtracted from the corresponding signal value in the odd path. This corresponds to high-pass filtering in a conventional filter bank. The prediction error acts as input for a so-called update step U, whose output is added to the values of the even path. This corresponds to a low-pass filter and is essential for the suppression of aliasing components in the low-pass band. The mapping of integer signal values to integer sub-band values is called Integer Wavelet Transform (IWT) and is simply achieved by rounding the output values of the prediction and update modules to integer values [6].

The lifting scheme, however, is not only suitable for the design of dyadic decompositions, but also for non-dyadic ones, i.e. for the design of M-channel filter banks. While the design of M-channel wavelet filter banks has been subject of research projects for many years (e.g. [7, 8, 9, 10, 11, 12]), the design of M-band decompositions performing an integer wavelet transform has not, to the author's knowledge, been addressed in the literature before.

This paper introduces a new design method for IWT 3-channel filter banks based on the lifting scheme. The design offers a way of handling signal boundaries with the minimum of computational complexity. The integer-to-integer mapping enables the application of the transform to lossless image data compression.

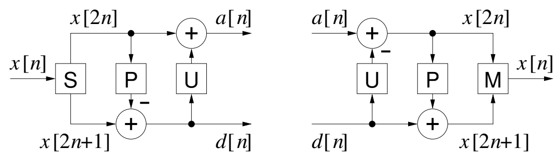

Fig. 1. Signal decomposition (left) and reconstruction (right) in a conventional lifting scheme

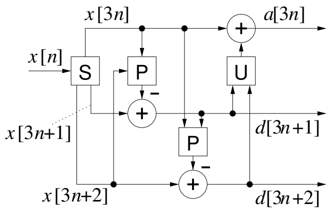

Fig. 2. Signal decomposition in a three-channel lifting scheme

2. PROPOSED LIFTING STRUCTURE

Figure 2 shows the major difference of the new decomposition scheme in comparison to dyadic lifting schemes (Fig.1). The incoming signal is split into three sub-signals instead of two allowing the application of two prediction steps.

The operations of prediction and update can be more clearly visualised with the aid of flow diagrams. Figure 3 gives an example for the decomposition and reconstruction of a signal of length $N = 9$. The first prediction step (i.e. high-pass filter) uses signal values x_n weighted by the coefficients β_1 - β_4. The resulting prediction error values are $d_1, d_3, \ldots$ (detail signal 1). The second prediction step utilises original signal values as well as the output of the first prediction step using the coefficients α_1 - α_4 and results to detail coefficients d_0, d_2, and so on. The update step is also based on four coefficients (γ_1 - γ_4) in this design example and includes the output values of both prediction steps. It outputs values from the low-pass channel, i.e. the approximation values $a_{n/3}$. The synthesis stage (Fig. 3, bottom) simply inverts all operations.

As can be seen in Fig.3, the processing steps lack input values at the signal boundaries. We propose to use zero as input where the input corresponds to a prediction error (or detail value), as for example at the left signal boundary. If an original signal value is required, a value must be chosen that provides the best extrapolation

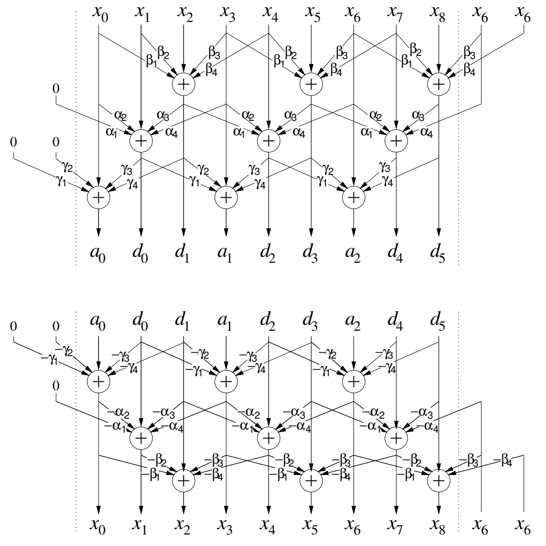

Fig. 3. Signal flow in signal analysis (top) and synthesis (bottom) with exception handling at signal boundaries for signals with length N and $(N \bmod 3) = 0$

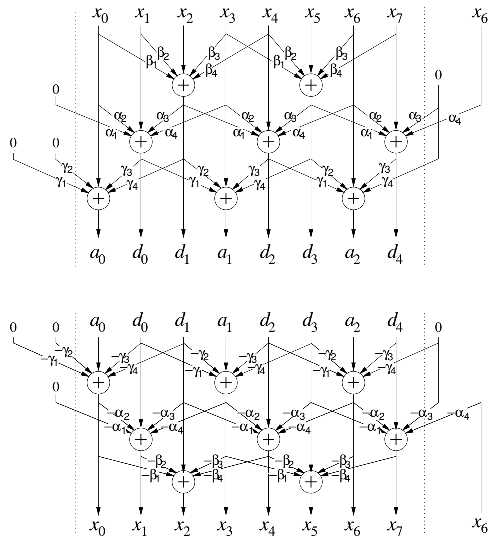

Fig. 4. Signal flow in signal analysis (top) and synthesis (bottom) with exception handling at signal boundaries for signals with length N and $(N \bmod 3) = 2$

of the signal and is available for signal reconstruction in the synthesis stage. Inspecting the flow diagram carefully, it becomes obvious, for example, that x_7 and x_8 cannot be used to reconstruct x_7 from d_4, because they are not available yet. So, x_6 is the best choice.

Figure 4 shows how the exception handling changes if the signal is shorter by one value $(N \bmod 3) = 2$. The handling for $(N \bmod 3) = 1$ can be derived accordingly.

The impulse responses of the six filters of the corresponding three-channel filter bank can be identified according to the explanations in [13]. The analysis high-pass filters are

$$\begin{aligned} h_1[n] &= \{\alpha_1\beta_1 \;\; \alpha_1\beta_2 \;\; \alpha_1 \;\; (\alpha_1\beta_3 + \alpha_2 + \alpha_3\beta_1) \\ &\qquad (\alpha_1\beta_4 + 1 + \alpha_3\beta_2) \;\; \alpha_3 \;\; (\alpha_3\beta_3 + \alpha_4) \;\; \alpha_3\beta_4\,\} \\ h_2[n] &= \{\beta_1 \;\; \beta_2 \;\; 1 \;\; \beta_3 \;\; \beta_4\}\,. \end{aligned}$$

The analysis low-pass filter is

$$\begin{aligned} h_0[n] = \Big\{ & (\alpha_1\beta_1\gamma_1) \;\; (\alpha_1\beta_2\gamma_1) \;\; (\alpha_1\gamma_1) \\ & [\alpha_1\beta_3\gamma_1 + \alpha_2\gamma_1 + \beta_1\cdot(\alpha_3\gamma_1 + \gamma_2 + \alpha_1\gamma_3)] \\ & [\alpha_1\beta_4\gamma_1 + \gamma_1 + \beta_2\cdot(\alpha_3\gamma_1 + \gamma_2 + \alpha_1\gamma_3)] \\ & (\alpha_3\gamma_1 + \gamma_2 + \alpha_1\gamma_3) \\ & [\beta_3\cdot(\alpha_3\gamma_1 + \gamma_2 + \alpha_1\gamma_3) + \alpha_4\gamma_1 + 1 + \\ & \qquad \alpha_2\gamma_3 + \beta_1\cdot(\gamma_4 + \alpha_3\gamma_3)] \\ & [\beta_4\cdot(\alpha_3\gamma_1 + \gamma_2 + \alpha_1\gamma_3) + \gamma_3 + \beta_2\cdot(\gamma_4 + \alpha_3\gamma_3)] \\ & (\gamma_4 + \alpha_3\gamma_3) \;\; (\alpha_3\beta_3\gamma_3 + \beta_3\gamma_4 + \alpha_4\gamma_3) \\ & \beta_4\cdot(\gamma_4 + \alpha_3\gamma_3)\Big\}\;, \end{aligned}$$

i.e. the analysis stage of the three-channel filter bank consists of finite impulse response (FIR) filters with eight, five, and eleven taps.

The impulse responses of the synthesis filters with 2×10 and 7 taps are accordingly

$$\begin{aligned} g_1[n] = \Big\{ & -\gamma_3\alpha_4\beta_4 \;\; 0 \;\; \gamma_3\alpha_4 \\ & [-\gamma_3\cdot(\alpha_4\beta_2 - \beta_3 + \alpha_2\beta_4) - \beta_4 - \gamma_1\alpha_4\beta_4] \\ & -\gamma_3 \;\; (\gamma_3\alpha_2 + 1 + \gamma_1\alpha_4) \\ & [\beta_1\gamma_3 - \beta_2\cdot(\gamma_3\alpha_2 + 1 + \gamma_1\alpha_4) + \beta_3\gamma_1 - \beta_4\alpha_2\gamma_1] \\ & -\gamma_1 \;\; \gamma_1\alpha_2 \;\; \gamma_1\cdot(\beta_1 - \alpha_2\beta_2)\Big\} \\ g_2[n] = \Big\{ & -\gamma_4\alpha_4\beta_4 \;\; 0 \;\; \gamma_4\alpha_4 \\ & [-\gamma_4\cdot(\alpha_4\beta_2 - \beta_3 + \alpha_2\beta_4) + \alpha_3\beta_4 - \gamma_2\alpha_4\beta_4] \\ & -\gamma_4 \;\; (\gamma_4\alpha_2 - \alpha_3 + \gamma_2\alpha_4) \\ & [\beta_1\gamma_4 - \beta_2\cdot(\gamma_4\alpha_2 - \alpha_3 + \gamma_2\alpha_4) + 1 + \\ & \qquad \beta_3\gamma_2 - \beta_4\cdot(\alpha_2\gamma_2 - \alpha_1)] \\ & -\gamma_2 \;\; (\gamma_2\alpha_2 - \alpha_1) \;\; [\gamma_2\cdot(\beta_1 - \alpha_2\beta_2) + \alpha_1\beta_2]\Big\} \\ g_0[n] = \Big\{ & \alpha_4\beta_4 \;\; 0 \;\; -\alpha_4 \;\; (\alpha_4\beta_2 - \beta_3 + \alpha_2\beta_4) \;\; 1 \\ & \qquad -\alpha_2 \;\; (\alpha_2\beta_2 - \beta_1)\Big\}\;. \end{aligned}$$

The integer-to-integer mapping is simply achieved by rounding the results after each lifting step. For example, the operations for filter $h_2[n]$ are with $n = (3m+1)/2$

$$\begin{aligned} d_m &= x_n + \lfloor \beta_1\cdot x_{n-2} + \beta_2\cdot x_{n-1} + \\ &\qquad \beta_3\cdot x_{n+1} + \beta_4\cdot x_{n+2} + 0.5\rfloor\;. \end{aligned}$$

The impulse responses above look more or less complicated. They enable, however, a relatively simple design as explained in the next section.

3. FILTER DESIGN

3.1. Basic requirements

In general, any arbitrarily chosen set of weightings α_i, β_i and γ_i would lead to filter banks with perfect reconstruction. Having the application of lossless image data compression in mind, however, we are interested in a filter bank with maximum compaction of signal energy. Thus, the filters $h_1[n]$ and $h_2[n]$ must be real high-pass filters. Let

$$H(z) = \sum_{n=0}^{t-1} h[n] \cdot z^n \tag{1}$$

be the frequency response (in z-domain) of a t-tap filter $h[n]$. Then $H_1(z)|_{z=1} = 0$ and $H_2(z)|_{z=1} = 0$ must hold. This leads to following conditions

$$0 = \beta_1 + \beta_2 + 1 + \beta_3 + \beta_4 \quad \text{and} \tag{2}$$

$$0 = 1 + \alpha_2 + \alpha_4 \; . \tag{3}$$

Furthermore, $h_0[n]$ should be a real low-pass filter, i.e. $H_0(z)|_{z=-1} = 0$ leading to

$$\begin{aligned} 0 = (\gamma_1 - \gamma_3) \cdot \\ & [(\alpha_1 - \alpha_3) \cdot (\beta_1 - \beta_2 + 1 - \beta_3 + \beta_4) + 1 + \alpha_4 - \alpha_2] \\ & +(\gamma_4 - \gamma_2) \cdot (\beta_1 - \beta_2 + 1 - \beta_3 + \beta_4) + 1 \; . \end{aligned} \tag{4}$$

$g_1[n]$ and $g_2[n]$ are forced to be true high-pass filters by following conditions

$$\begin{aligned} 0 = (\gamma_1 + \gamma_3) \cdot [(\alpha_2 + \alpha_4) \cdot (1 - \beta_2 - \beta_4) - 1 + \beta_1 + \beta_3] \\ +1 - \beta_2 - \beta_4 \end{aligned} \tag{5}$$

$$\begin{aligned} 0 = (\gamma_2 + \gamma_4) \cdot [(\alpha_2 + \alpha_4) \cdot (1 - \beta_2 - \beta_4) - 1 + \beta_1 + \beta_3] \\ -(\alpha_1 + \alpha_3) \cdot (1 - \beta_2 - \beta_4) + 1 \; . \end{aligned} \tag{6}$$

$g_0[n]$ is not set to a real low pass, since this contradicts one of the desired properties discussed in next subsection.

3.2. Selection of useful filter properties

So far, only five conditions have been formulated for the determination of twelve variables.

The wavelet filters that are most successful in image data compression are based on a design putting a maximum number of zeros (vanishing moments) at $z = 1$ (high pass) or $z = -1$ (low pass) in order to force maximum flat frequency responses [14, 15]. Zeros at $z = 1$ are in accordance with the frequency characteristic of natural images such as photographs, which typically have a strong peak at low frequencies. Frequency parts close to the normalised[1] frequency of 0.5 are mostly caused by the noise floor. With respect to equation (1), multiple vanishing moments at $z = 1$ can be incorporated by setting $z = \sqrt[n]{n^p}$ $(p = 0, 1, 2, \ldots)$. The second zero for $h_2[n]$, for example, is included using $z = \sqrt[n]{n}$ leading to the condition

$$0 = 0 \cdot \beta_1 + 1 \cdot \beta_2 + 2 \cdot 1 + 3 \cdot \beta_3 + 4 \cdot \beta_4 \tag{7}$$

A different interpretation of this approach is based on the approximation of signal segments by polynomials of increasing order [16].

In the case of $h_2[n]$, the maximum number of zeros is obtained by the conditions (2), (7) and the following two

$$0 = 0 \cdot \beta_1 + 1 \cdot \beta_2 + 4 \cdot 1 + 9 \cdot \beta_3 + 16 \cdot \beta_4 \tag{8}$$

$$0 = 0 \cdot \beta_1 + 1 \cdot \beta_2 + 8 \cdot 1 + 27 \cdot \beta_3 + 64 \cdot \beta_4 \; . \tag{9}$$

[1] normalised by the sampling frequency

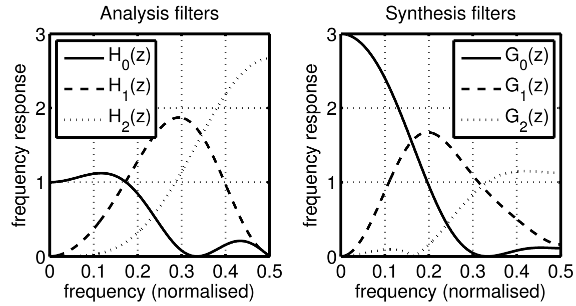

Fig. 5. Spectra of the filters of the proposed three-channel filter bank

One additional vanishing moment is assigned to each of the filters $h_1[n]$ and $g_1[n]$. The corresponding conditions are in this order:

$$\begin{aligned} 0 = \; & 0 \cdot \alpha_1\beta_1 + 1 \cdot \alpha_1\beta_2 + 2 \cdot \alpha_1 + \\ & 3 \cdot (\alpha_1\beta_3 + \alpha_2 + \alpha_3\beta_1) + 4 \cdot (\alpha_1\beta_4 + 1 + \alpha_3\beta_2) + \\ & 5 \cdot \alpha_3 + 6 \cdot (\alpha_3\beta_3 + \alpha_4) + 7 \cdot \alpha_3\beta_4 \end{aligned} \tag{10}$$

and

$$\begin{aligned} 0 = \; & 0 \cdot (-\gamma_3\alpha_2\beta_4) + 1 \cdot 0 + 2 \cdot \gamma_3\alpha_4 + \\ & 3 \cdot [-\gamma_3 \cdot (\alpha_4\beta_2 - \beta_3 + \alpha_2\beta_4) - \beta_4 - \gamma_1\alpha_4\beta_4] \\ & 4 \cdot (-\gamma_3) + 5 \cdot (\gamma_3\alpha_2{+}1{+}\gamma_1\alpha_4) + \\ & 6 \cdot [\beta_1\gamma_3 - \beta_2 \cdot (\gamma_3\alpha_2{+}1{+}\gamma_1\alpha_4) + \beta_3\gamma_1 - \beta_4\alpha_2\gamma_1] - \\ & 7 \cdot \gamma_1 + 8 \cdot \gamma_1\alpha_2 + 9 \cdot \gamma_1 \cdot (\beta_1 - \alpha_2\beta_2) \end{aligned} \tag{11}$$

In order to propagate as little as possible of the signal energy through the analysis filters, one degree of freedom is used to put a zero at $z = -1$ for $H_1(z)$ and filter $h_1[n]$ is becoming a band-pass

$$\begin{aligned} 0 = \; & \alpha_1\beta_1 - \alpha_1\beta_2 + \alpha_1 - \\ & (\alpha_1\beta_3 + \alpha_2 + \alpha_3\beta_1) + (\alpha_1\beta_4 + 1 + \alpha_3\beta_2) - \\ & \alpha_3 + (\alpha_3\beta_3 + \alpha_4) - \alpha_3\beta_4 \; . \end{aligned} \tag{12}$$

The non-linear equation system consisting of the eleven conditions (2) - (12) leads to following rational solution with one degree of freedom

$$\begin{aligned} \alpha_1 &= -\frac{7}{24} - 2 \cdot \gamma_4 \quad \alpha_2 = -\frac{2}{3} \quad \alpha_3 = \frac{5}{24} - 2 \cdot \gamma_4 \quad \alpha_4 = -\frac{1}{3} \\ \beta_1 &= \frac{1}{6} \quad \beta_2 = -\frac{2}{3} \quad \beta_3 = -\frac{2}{3} \quad \beta_4 = \frac{1}{6} \\ \gamma_1 &= \frac{5}{18} \quad \gamma_2 = \frac{3}{8} + \gamma_4 \quad \gamma_3 = \frac{2}{9} \quad \gamma_4 = ? \; . \end{aligned} \tag{13}$$

Which value should be assigned to γ_4? $\gamma_4 = -53/480$ would introduce a second zero at $z = -1$ for $H_0(z)$ and $\gamma_4 = 1/48$ a second zero at $z = -1$ for $H_1(z)$. With respect to the typical characteristics of images, both do not lead to improved compression results. $\gamma_4 = -7/480$ introduces a second zero at $z = 1$ for $G_2(z)$ simultaneously forcing a second zero in $H_0(z)$ at a normalised frequency of $1/3$. At this position, images contain more energy to be cancelled out than at $1/2$. Investigations have shown that it is advantageous to move these zeros slightly apart from each other by choosing $\gamma_4 = -10/480$ instead. Figure 5 shows the resulting frequency responses.

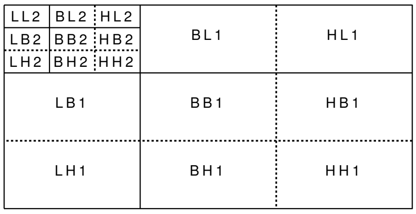

Fig. 6. Structure of a transformed image after two non-dyadic decomposition steps (H ... high-pass filtered, B ... band-pass filtered, L ... low-pass filtered)

Table 1. Results of lossless compression in bits per pixel

image	5/3	11/8/5	difference
barbara.y.pgm	4.594	4.502	0.092
barbara2.y.pgm	4.778	4.776	0.002
black.y.pgm	3.765	3.757	0.008
boats.y.pgm	4.057	4.030	0.026
goldhill.y.pgm	4.593	4.609	-0.016
zelda.y.pgm	3.870	3.856	0.014
cats_g.pgm	2.542	2.521	0.021
bike.pgm	4.364	4.405	-0.041
ct.pgm	3.287	3.381	-0.094
educ.pgm	4.534	4.432	0.102
average	4.038	4.027	0.011

4. APPLICATION AND DISCUSSION

The described filter bank has been implemented in a framework for image data compression performing similar operation as JPEG2000. Figure 6 depicts the decomposition structure of a transformed image with two decomposition steps. The encoder module treats the detail signals enclosed by the solid lines together as single sub-bands. The components BL1 and HL1, for example, belong to the same sub-band. Table 1 contains the compression results in bits per pixel for a selection of different grey-scale images. Barbara - Zelda are taken from [17], the other from [18]. The column '5/3' indicates the results when using the 5/3-wavelet filter as defined in [1], '11/8/5' the results when applying the filter bank based on the design method described above. The compression ratios are close to each other with some advantage for the newly designed filter bank.

There are two reasons why the new filter bank does not perform significantly better than 5/3 wavelet filters. First, the prediction performance (suppression of low frequencies) of $h_1[n]$ is rather poor and cancels out the advantage of $h_2[n]$ to a certain extent. Secondly, the effects of non-linearity owing to the rounding operations inside the prediction and update modules are lower in the 5/3 filter bank. This is because of the favourable factors of -0.5 in its first lifting step, and because the 5/3 sub-bands are affected by rounding in fewer lifting steps. Rounding deteriorates the filter characteristics depending on the values of the input signal and significantly reduces the possible compression ratio.

5. SUMMARY

In this paper, a novel method for the design of integer three-channel filter banks has been presented. Based on the lifting scheme a system of non-linear equations could be derived enabling the determination of all necessary lifting coefficients, i.e. impulse responses. The design constraints have been chosen with respect to the desired application in lossless image compression leading to competitive compression results. Future research will concentrate on possible compression performance improvements by shifting a pair of zeros of $H_2(z)$ along the unit circle.

6. REFERENCES

[1] ISO/IEC JTC1/SC29/WG11 N1890, *Information technology – JPEG 2000 Image Coding System*. JPEG 2000 Part I, Final Draft International Standard 15444, 25 Sep 2000

[2] Mallat, S.G.: A Theory for Multiresolution Signal Decomposition: The Wavelet Representation. *IEEE Trans. on Patt. Anal. and Mach. Intell.*, Vol.11, No.7, 1989, 674–693

[3] Strang, G.; Nguyen, T.: *Wavelets and Filter Banks*, Wellesley-Cambridge Press, 1996

[4] Sweldens, W.: The Lifting Scheme: A New Philosophy in Biorthogonal Wavelet Construction. *Proceedings of SPIE*, July 1995, Vol.2569, San Diego, USA, 68–79

[5] Daubechies, I.; Sweldens, W.: Factoring Wavelet Transform into Lifting Steps. *J. Fourier Anal. Appl.*, Vol.4, No.3, 1998, 247–269

[6] Calderbank, A.R.; Daubechies, I.; Sweldens, W.; Yeo, B.L.: Wavelet transform that maps integers to integers. *Appl. Comp. Harm. Anal.*, Vol.5, No.3, 1998, 332–369

[7] Zou, H.; Tewfik, A.H.: Discrete orthogonal M-band wavelet decompositions. *IEEE Int. Conf. on Acoustics, Speech, and Signal Proc. ICASSP-92*, 23-26 Mar 1992, Vol.4, 605–608

[8] Steffen, P.; Heller, P.N.; Gopinath, R.A.; Burrus, C.S.: Theory of regular M-band wavelet bases. *IEEE Trans. on Signal Proc.*, Vol.41, No.12, Dec 1993, 3497–3511

[9] Alkin, O.; Caglar, H.: Design of efficient M-band coders with linear-phase and perfect-reconstruction properties. *IEEE Trans. on Signal Proc.*, Jul 1995, Vol.43, No.7, 1579–1590

[10] Tran, T.D.: M-channel linear phase perfect reconstruction filter bank with rational coefficients. *IEEE Trans. on Circ. and Syst. I: Fund. Theory and Appl.*, Jul 2002, Vol.49, No.7, 914–927

[11] Chen, Y.-J.; Amaratunga, K.S.: M-channel lifting factorization of perfect reconstruction filter banks and reversible M-band wavelet transforms. *IEEE Trans. on Circ. and Syst. II: Anal. and Dig. Signal Proc.*, Dec 2003, Vol.50, No.12, 963–976

[12] Kofidis, E.; Designing *N*-band biorthogonal FIR systems given several of the analysis and synthesis filters. *Signal Processing*, Elsevier, Vol.85, No.7, July 2005, 1335–1351

[13] Strutz, T.; Müller, E.: Construction of semi-recursive PR-filter banks via generalised lifting. *Signal Processing*, Elsevier, Vol.84, 2004, 77–93

[14] Daubechies, I.: Orthonormal Bases of Compactly Supported Wavelets. *Communications on Pure and Applied Mathematics*, Vol.41, 1988, 909–996

[15] Antonini, M.; Barlaud, M.; Mathieu, P.; Daubechies, I.: Image Coding Using Wavelet Transform. *IEEE Trans. on Image Proc.*, Vol.1, No.2, April 1992, 205–220

[16] Strutz, T.; Müller, E.: Wavelet filter design for image compression. *IEEE-SP International Symposium on Time-Frequency and Time-Scale Analysis*, Paris, 18-21 Jun 1996, 273–276

[17] http://www.bath.ac.uk/elec-eng/research/sipg/resource /images.htm, last visited at 9 January 2009

[18] ITU-T Recommendation T.24: *Standardized digitized image set*, Version 3, 1998